

# Impact of Urban Expansion On Carbon Storage Under Multi-Scenario Simulations In Wuhan, China

Zhuo Wang (✉ [fortleisure@cug.edu.cn](mailto:fortleisure@cug.edu.cn))

China University of Geosciences

Jie Zeng

China University of Geosciences <https://orcid.org/0000-0002-2714-6187>

Wanxu Chen

China University of Geosciences


---

## Research Article

**Keywords:** Urban expansion, Terrestrial carbon storage, Multi-scenario simulation, PLUS model, InVEST model, Wuhan, China

**Posted Date:** December 20th, 2021

**DOI:** <https://doi.org/10.21203/rs.3.rs-1129892/v1>

**License:**  This work is licensed under a Creative Commons Attribution 4.0 International License. [Read Full License](#)

---

**Version of Record:** A version of this preprint was published at Environmental Science and Pollution Research on February 11th, 2022. See the published version at <https://doi.org/10.1007/s11356-022-19146-6>.

# Abstract

Carbon storage in terrestrial ecosystems, which is the basis of the global carbon cycle, reflects the changes in the environment due to anthropogenic impacts. Rapid and effective assessment of the impact of urban expansion on carbon reserves is vital for the sustainable development of urban ecosystems. Previous studies lack research regarding different scenarios during future city and comprehensive analysis on the driving factors from the socioeconomic point of view. Therefore, this study examined Wuhan, China and explored the latent effects of urban expansion on terrestrial carbon storage by combining the Integrated Valuation of Ecosystem Services and Trade-offs (InVEST) and Patch-generating Land Use Simulation (PLUS) model. Based on different socioeconomic strategies, we developed three future scenarios, including Baseline Scenario (BS), Cropland Protection Scenario (CP), and Ecological protection Scenario (EP), to predict the urban built-up land use change from 2015 to 2035 in Wuhan and discussed the carbon storage impacts of urban expansion. The result shows that: (1) Wuhan's urban built-up land area expanded 2.67 times between 1980 and 2015, which is approximately 685.17 km<sup>2</sup> and is expected to continuously expand to 1,349–1,945.01 km<sup>2</sup> by 2035. (2) Urban expansion in Wuhan has caused carbon storage loss by 5.12×10<sup>6</sup> t during 1980–2015 and will lead to carbon storage loss by 6.15×10<sup>6</sup> t, 4.7×10<sup>6</sup> t, and 4.05×10<sup>6</sup> t under BS, CP, and EP scenarios from 2015 to 2035, accounting for 85.42%, 81.74%, and 78.79% of the total carbon loss, respectively. (3) The occupation of cropland by urban expansion is closely related to the road system expansion, which is the main driver of carbon storage reduction from 2015 to 2035. (4) We expect that by 2035, the districts facing carbon loss caused by the growth of urban built-up land will expand outward around secondary roads, and the scale of outward expansion under various scenarios will be ranked as: BS > CP > EP. In combination, the InVEST and the PLUS model can assess the impact of urban expansion on carbon storage more efficiently and is conducive to carrying out urban planning and promoting a dynamic balance between urban economic development and human well-being.

## 1. Introduction

Enhancing the carbon sequestration function of terrestrial ecosystems is essential to reducing carbon emissions and addressing the major challenges of climate warming (Fang et al., 2015; Yang et al., 2020). The impact of land use change on the dramatic increase of atmospheric CO<sub>2</sub> concentration is second only to fossil energy burning. Moreover, it markedly influences carbon storage in terrestrial ecosystems (Chuai et al., 2011; Stuiver, 1978; Tang and Peng, 2018). As the most drastic land use change in the process of rapid urbanisation and industrialisation (He et al., 2016), urban expansion led a large number of ecological lands (e.g. cropland, forest land, and grassland) to be transformed into urban construction land (Feng et al., 2020; Sallustio et al., 2015). This process directly caused the loss of high carbon density land (Wu et al., 2016) and altered the process, structure, and function of the natural ecosystem (Baumann et al., 2016; Houghton et al., 2012). Consequently, urban expansion significantly reduced carbon storage in terrestrial ecosystems and further affected the global carbon cycle and urban sustainability. Therefore, a scientific evaluation of the influence of urban expansion on carbon reserve is conducive to understanding carbon storage change in an urban ecosystem. Furthermore, it is of great significance to urban ecosystem protection and sustainable urban development.

Previous studies have linked land use simulation models and carbon storage evaluation models to assess the potential impacts of future urban expansion on carbon storage from different perspectives. For example, Wang et al. (2018) adopted the MLP (Multi-layer Perceptron) and the Integrated Valuation of Ecosystem Services and Trade-offs (InVEST) model to simulate the future land use of the Three Gorges Reservoir, and their results showed

that terrestrial carbon storage reductions are consistent with urban expansion. Lahiji et al. (2020) combined the scenario-based multi-objective land allocation program with the InVEST model to investigate the carbon storage change under different land use policies in the agroforestry landscape of northern Iran. Notably, most land-use simulation models used in conjunction with InVEST models are based on cellular automata (CA). For example, Liang et al. (2021) and Sadat et al. (2020) integrated Markov-CA model and the InVEST model to evaluate the impact of future land use changes on regional terrestrial ecosystem carbon storage in the Loess Plateau and Qaem Shahr County of northern Iran. He et al. (2016) evaluated the potential effects of urban expansion on regional carbon storage in Beijing based on LUSD-urban (Land Use Scenario Dynamics-urban) and the InVEST model. Lyu et al. (2019) analysed the impact of urbanisation on carbon storage under different policies in Shizuishan City, China, using SLEUTH-3r (the 3r version of Slope, Land use, Exclusion, Urban extent, Transportation and Hillshade model) and the InVEST model. Deng et al. (2020), Liu et al. (2019), and Gao and Wang (2019) coupled FLUS (Future Land Use Simulation) and the InVEST model to analyse how dynamic changes in future land use influence carbon storage.

Among these, the InVEST model has been widely used owing to its effectiveness in revealing the relationships between land-use/cover change and carbon storage change (Maanan et al., 2019; Yang et al., 2020; Zhao et al., 2018). Meanwhile, CA-based land use simulation models are useful tools for predicting future urban land expansion (Deng, 2020; Liang, 2018; Liu, 2017). However, these simulation models do not easily reveal the potential driving factors of land use change (Sohl and Claggett, 2013) or capture the temporal-spatial evolution of various land use patches (Meentemeyer et al., 2013; Yang et al., 2020). Contrastingly, the Patch-generating Land Use Simulation (PLUS) model can better tap into the incentives of various types of land use changes by using a new analysis strategy—Land Expansion Analysis Strategy (LEAS) and can better emulate the patch-level changes of various types of land use by utilising a new seed growth mechanism—a CA model based on multi-type Random Seeds (CARS). Depend on LEAS and CARS module (Liang et al., 2021), PLUS can more accurately analyse the influence of urban growth on the carbon reserve in terrestrial ecosystems under different simulated future scenarios.

This study took the rapidly expanding city of Wuhan as an example to explore how much urban sprawl affects carbon stocks based on the PLUS and InVEST models. Wuhan is a megacity in central China which possesses an integrated transportation hub. It has seen a rapid increase in urbanisation levels from 49.54% in 1980 (He, 2004) to 79.41% in 2015, during which time urban populations also increased. Concurrently, being one of China's "Low-carbon City" and "Resource-saving and Environment-friendly" pilot cities, Wuhan proposed the *Wuhan City Carbon Emission Peak Action Plan (2017-2022)*. Naturally, Wuhan needs to realise the sustainable management of the urban ecosystem to ensure the continuous improvement of the regional ecological environment and achieve the dynamic balance of accelerating regional, social, and economic development.

To clearly reveal the spatiotemporal relationship between urban expansion and carbon storage in Wuhan, this study set the following three objectives: (1) to explore the spatio-temporal pattern characteristics and driving factors of urban expansion in Wuhan; (2) to analyse and predict the dynamic change trend of carbon storage of Wuhan's terrestrial ecosystems in the past and future; (3) to determine the impacts of past and future urban expansion on carbon storage in regional terrestrial systems and the resulting changes in economic value.

## 2. Material And Methods

## 2.1 Study area

As the capital city of Hubei Province, Wuhan has the fourth largest urban population in China. As of the end of 2020, Wuhan had a resident population of 12.33 million, and its regional gross domestic product that year was 1.56 trillion yuan. The total economic output ranked among the top ten cities in the country. Wuhan is one of the first branch of cities in China to explicitly put forward a quantified target for carbon emission peak. According to *Wuhan City Carbon Emission Peak Action Plan (2017-2022)*, Wuhan's carbon emissions will reach the peak, controlled at 173 million tons of carbon emissions by 2022.

According to the land use data of the Resources and Environmental Sciences Data Center (RESDC), Chinese Academy of Sciences (<http://www.resdc.cn>), the total surface area of Wuhan was 8,578.21 km<sup>2</sup> in 2015, with the main land use types being 4,624.3 km<sup>2</sup> of cropland and 1,611.42 km<sup>2</sup> of wetland.

## 2.2 Data sources and preprocessing

Data used for land use simulation and carbon storage calculation in this study are as follows: (1) the raster data of land use in Wuhan in 1980, 1995, 2005, and 2015 were obtained from RESDC (<http://www.resdc.cn>), whose remote sensing information sources are mainly Landsat-MSS/TM/ETM and Landsat 8 images covering the whole country. The land use types of this dataset are divided into six categories and 25 sub-categories (Chen et al., 2019; Liu et al., 2014), with a 30 m spatial resolution. By comparing the results from field survey and remote sensing, the total accuracy of this land use change data set for six land use categories reached 94.3%, while the total accuracy of 25 sub-categories reached 91.2% (Chen et al., 2020; Zeng et al., 2020). The DEM, slope, GDP, and population data were also collected from RESDC (<http://www.resdc.cn/>), in which the spatial resolution of DEM and slope data was 250 m, and that of GDP and population data was 1 km; (2) soil type data were obtained from National Tibetan Plateau Scientific Data Center, with a spatial resolution of 1 km (<http://westdc.westgis.ac.cn/zh-hans/>); (3) raster data for road networks were obtained from OpenStreetMap (<https://www.openstreetmap.org/>); (4) annual mean temperature and annual mean precipitation data were obtained from WorldClim with a spatial resolution of 30 s (<https://www.worldclim.org/>).

This study reclassified the original data and merged the 25 sub-categories of the original land use data to obtain eight land use types. The details can be seen in Appendix A.

## 2.3 Methods

In this study, a coupled PLUS and Markov model was used to execute dynamic simulations and make a prediction for land use. Afterwards, the change in carbon storage and the corresponding change in economic value were calculated based on the InVEST model. The advantage of the coupled PLUS-Markov model lies in integrating CA's ability to deal with the spatial changes of complex systems and Markov's ability to predict the amount of land, thus realising the full mining of the dynamic evolution of land use information in both space and quantity.

Overall experimental processes in this study are as follows (Figure 2). Firstly, land use data of 2005 and 2010 and driving factor data are input into the PLUS model to get the growth probabilities of each land use and simulated land use data in 2010. These were compared in the PLUS model to conduct an accuracy assessment. If the accuracy meets the requirements, the transition probability matrix obtained from the transition matrix data between 2005 and 2010 was used to calculate the 2035 land use under various scenarios. Finally, using 2005 land use data, growth probabilities of each land use and the 2035 land use under various scenarios are input into

the PLUS model to get the 2035 land use map under the baseline scenario (BS), cropland protection scenario (CP), and ecological protection scenario (EP). Based on the land use maps at different times and land use carbon pool tables, the map of changes in carbon storages can be obtained in the InVEST model.

## 2.2.1 Future urban expansion simulation

Herein, the coupled Markov and PLUS models were applied to emulate land use changes, in which the PLUS model was used to map land use under future scenarios and obtain the driving factor of land use change, and the Markov model was utilised to obtain the amount of land use under various future scenarios.

The Markov chain is characterised by its stability and as being “after effectless”, where “after effectless” refers to the state of a thing at a certain moment in the future which is not related to any previous state but only to the current state in the random development process; stability means that its change process tends to be stable. It can generate a land use transfer matrix through different periods of land use data and calculate the transfer probability matrix of land use change in the study area. Based on this, it can be used to predict the future amount of land use types in the study area.

Combined with *Wuhan City Land Use Overall Plan (2006–2020)*, *Wuhan Central City Lake Protection Plan (2004–2020)*, *Wuhan City Urban Planning Guiding Opinions in 2030*, *Wuhan City Master Plan (2017–2035)*, *National Land Use Overall Plan Outline (2006–2020)*, this study refers to previous research (Chen et al., 2020; Li et al., 2020; Lu et al., 2009; Wang et al., 2020) and recommendations from relevant experts to conduct appropriate adjustments to the transition probability matrix from 2005 to 2010. This study obtained the future land use amount of Wuhan under three different scenarios, which was used for the land use spatial simulation of the PLUS model. Finally, the following three future scenarios were set.

**Baseline scenario (BS):** Based on the development trend of land use from 2005 to 2010 and the Markov chain, the demand for land use under the historical development trend in 2035 was obtained.

**Cropland protection scenario (CP):** On the basis of BS, with reference to the *National Land Use Overall Plan Outline (2006–2020)* and *Wuhan City Land Use Overall Plan (2006–2020)*, cropland is protected, and the total amount of built-up land was strictly controlled to improve intensive utilisation of land. Therefore, the transfer probability of cropland to built-up land was reduced by 30%, and this was added to cropland.

**Ecological protection scenario (EP):** The aim of the EP scenario is to strengthen the protection of ecological lands such as grassland and forest land. Based on CP, the conversion of cropland, grassland, forest land, and wetland with ecological functions to built-up land was strictly controlled by referring to *Wuhan City Land Use Overall Plan (2006–2020)*. Under the EP scenario, the transfer probability of crop land to built-up land was reduced by 30%, and the reduction was added to the conversion of cropland to forest land; the transfer probability of grassland and forest land to built-up land was reduced by 40%, and this was added to grassland and forest land respectively. The transfer probability of wetland to built-up land was reduced by 30%, and this was added to forest land.

Finally, the Markov model was used to calculate the land use demand in three different scenarios; the specific quantities are shown in Table 1.

**Table 1** The number of demand pixels of each land use type under different scenarios in Wuhan in 2035 (units: pixel).

Various scenarios	Cropland	Forest land	Grassland	River	Wetland	Urban built-up land	Rural built-up land	Unused land
2035 BS	3,785,307	790,306	105,455	304,321	2,088,207	1,870,250	262,183	3,624
2035 CP	4,079,644	790,381	106,971	304,992	2,086,895	1,575,721	261,506	3,525
2035 EP	3,789,281	1,227,642	118,443	304,097	2,057,836	1,449,455	259,359	3,522

The PLUS model can emulate the future land use map and excavate the drivers of land use change. In addition, compared to other widely used urban expansion simulation models (Liu et al., 2017), PLUS is easy to operate.

The land use change is the result of the combined effects of various types of land's own physical and chemical conditions and natural, social, economic, and other internal and external factors. This study selected 15 driving factors (details can be found in Appendix B) such as population, GDP, soil type, elevation, the proximity to cities and towns, and so on.

To imitate the patch evolution of land use, the PLUS model adopts a multi-type random patch seeding mechanism based on decreasing threshold, which is realised through the calculation process of overall probability. Based on the Monte Carlo method, the growth probability surface ( $P_{i,k}^{d=1}$ ) for land use and overall probability ( $OP_{i,k}^{d=1,t}$ ) can be obtained when  $\Omega_{i,k}^t$  is 0.

$$OP_{i,k}^{d=1,t} = \begin{cases} P_{i,k}^{d=1} \times (r \times u_k) \times D_k^t, & \text{if } \Omega_{i,k}^t = 0 \text{ and } r < P_{i,k}^{d=1} \\ P_{i,k}^{d=1} \times \Omega_{i,k}^t \times D_k^t, & \text{all others} \end{cases} \quad (1)$$

Here,  $r$  takes values from 0 to 1;  $u_k$  is selected by the user, and represents the threshold for generating new land use patches for land use type  $k$ ;  $\Omega_{i,k}^t$  refers to the proportions that land use  $k$  account for the neighborhood of cell  $i$ ;  $D_k^t$  denotes the gap between the present land use amount and future land use demand at iteration  $t$ . If land use  $c$  wins the competition against land use  $k$ , the decreasing threshold  $\tau$  is used to evaluate the nominee land use  $c$  selected by the roulette wheel, as shown below:

$$\text{If } \sum_{k=1}^N |G_c^{t-1}| - \sum_{k=1}^N |G_c^t|$$

2

$$\begin{cases} \text{Change } P_{i,c}^{d=1} > \tau \text{ and } TM_{k,c} = 1 \\ \text{No change } P_{i,c}^{d=1} \leq \tau \text{ or } TM_{k,c} = 0 \end{cases} \quad \tau = \delta^l \times r1$$

3

where "Step" is used to approach the future land use demand;  $\delta$  is the attenuation factor;  $r1$  takes value between 0 to 2;  $l$  is the amount of attenuation steps; and  $TM_{k,c}$  is the transfer matrix of land use  $k$  to  $c$ , which is used to

determine if the conversion of land use  $k$  to land use  $c$  is permitted. Many parameters of the model in the practice come from the tutorial of the PLUS software.

In this study, a Kappa index and a Figure of Merit (FoM) index were applied to verify the analogue accuracy of the model. A Kappa index is a test method proposed by Cohen and J. (1960) to detect whether the classification results of remote sensing images are consistent by establishing an error matrix for land use data and image classification results. It was used in this study to test the consistency between the analogue results and the current situation. The Kappa coefficient is calculated as follows:

$$Kappa = \frac{OA_O - OA_E}{(1 - OA_E)}, OA_O = \left( \sum_{k=1}^n OA_{kk} \right) / N(4)$$

where  $OA_O$  is the overall accuracy (OA) of the classification, representing the probability that the simulation result is consistent with the land use data for each random sample;  $OA_E$  indicates the probability that the simulation result caused by chance coincides with the current land use data;  $n$  is the total types of land use,  $N$  is the total number of samples;  $OA_{kk}$  is the number of samples correctly classified for the  $k$ -th land use type. The Kappa coefficient takes values from -1 to 1, where a higher value reflects a more accurate model.

FoM is used to better describe the accuracy of land use simulation than the Kappa coefficient (Pontius et al., 2008; Pontius and Millones, 2011). Its calculation equation is as follows:

$$FoM = \frac{1}{\max\{N_e, N_d\}} \sum_{k=1}^{N_d} \frac{1}{(1 + \beta d(k)^2)} (5)$$

where  $N_e$  represents the pixel amount of the simulated land use,  $N_d$  represents the pixel amount of the actual land use;  $\beta$  is a scale factor greater than 0, usually 1/9;  $d(k)$  is the distance between the  $k$ -th detected actual land use current pixel and the nearest simulation pixel. Generally speaking, the FoM values are within 0.3. In practice, FoM usually takes values between 0.1 and 0.2 (Chen et al., 2014), which indicates that it is of relatively high accuracy.

The accuracy of the PLUS model determines the result of the experiment. Based on the land use data of Wuhan in 2005 and 2010, and the 15 driving factors, we employed PLUS to emulate the land use of Wuhan in 2010. After comparing the simulated land use with the actual in 2010, using PLUS, we found that when sampling rate was 5%, the Kappa coefficient was 0.87, the OA index was 0.917, and the FoM was 0.205, indicating that the model was of high accuracy and can be applied to the requirements of this study for the following simulation.

## 2.2.2 Carbon storage assessment

The InVEST model is suitable for calculating the carbon storage of the terrestrial ecosystem in the study area. Composed of land, freshwater and ocean modules, this model is used to evaluate the service functions of ecosystems and their economic value and support ecosystem management and decision-making. The carbon storage assessment model derives from the land module. According to this model, most of the existing carbon storage in the environment relies on four basic carbon pools: above-ground biomass, underground biomass, soil, and dead organic matter. The calculation equation is as follows:

$$C_i = C_{i\_above} + C_{i\_below} + C_{i\_soil} + C_{i\_dead}(6)$$

$$C_{total} = \sum_{i=1}^n (A_i \times C_i)(7)$$

where  $C_i$  is the carbon density of the  $i$ -th type of land use;  $C_{i\_above}$ ,  $C_{i\_below}$ ,  $C_{i\_soil}$  and  $C_{i\_dead}$  are the carbon densities of aboveground biomass, underground biomass, soil, and dead organic matter in the  $i$ -th type of land use, respectively;  $C_{total}$  is the total carbon storage in the study area;  $C_i$  is the carbon density of the  $i$ -th type of land use;  $A_i$  is the area of the  $i$ -th type of land use; and  $n$  is the number of land use types in the study area.

The carbon density data of each land use type needed for carbon storage calculation were mainly derived from the literature related to carbon density. Carbon density data is regionally specific. Based on the existing literature on carbon density of different regions, this study obtained the carbon density data of Hubei Province (seen in Appendix C) from Ke and Tang (2019), which had a smaller application scope and a higher accuracy in the study of specific regions compared with the carbon density data in other literature. As such, less error is generated in the calculation of Wuhan's carbon storage.

The calculation of the economic value of carbon storage requires three important parameters: (1) The value of carbon sequestration per ton ( $V$  in equation 8), where the social cost of carbon is recommended by the InVEST model; (2) the market discount rate ( $r$  in equation 8) reflects the phenomenon that current immediate benefits are preferred to future benefits in society; and (3) the inter-annual change rate of the carbon price ( $c$  in equation 8), which aims to adjust the value of carbon sequestration under the influence of changes in related losses under expected climate change. For plot  $x$ , the value of carbon storage change over a period of time is estimated by equation 8:

$$value_{seq_x} = V \frac{sequest_x}{yr_{fut} - yr_{cur}} \sum_{t=0}^{yr_{fut} - yr_{cur} - 1} \frac{1}{\left(1 + \frac{r}{100}\right)^t \left(1 + \frac{c}{100}\right)^t} (8)$$

where  $value_{seq_x}$  denotes the economic value of carbon sequestration under current and future land use change scenarios;  $x$  represents the carbon sequestration grid;  $V$  represents the value of carbon sequestration (t/USD);  $r$  represents the market discount rate (%);  $t$  represents the annual change rate (%) of the value of carbon sequestration per ton;  $yr_{cur}$  represents the terrestrial ecosystem carbon storage under the current land use scenario;  $yr_{fut}$  represents the carbon storage of terrestrial ecosystem under the future land use scenario; and  $sequest_x$  represents the amount of carbon sink or carbon loss in each grid under current and future land use scenarios. Tian et al. (2019) indicated that the current social cost of carbon emissions in China should be 9.20 \$/(t C), and according to the user instruction manual of the InVEST model, the Asian Development Bank uses a discount rate of 10–12% when evaluating projects (Sharp et al., 2015). In this study, the market discount rate of the economic value of carbon sinks between 2015–2035 is determined to be 10%. The interannual change rate of the social cost of carbon is set as unchanged, 0, by referring to relevant studies (Deng et al., 2020).

### 3. Results



### 3.1 Spatio-temporal pattern of urban expansion in Wuhan

Urban expansion and intense urban sprawl from 1980 to 2015 caused significant changes in Wuhan's land use. The area of urban built-up land increased from 256.66 km<sup>2</sup> in 1980 to 941.83 km<sup>2</sup> in 2015, depicting an increase of 266.96%. The rural built-up land reached a peak of 263.47 km<sup>2</sup> in 2005, and finally decreased to 257.35 km<sup>2</sup> in 2015 (higher than 239.48 km<sup>2</sup> in 1980), keeping a balance around a certain level (Figure 3). Wuhan's urban built-up land was mainly concentrated in the central plain area, with a trend of spreading from the centre to the surroundings, and mainly expanding to the south (Figure 4).

Between 1980 and 2015, a total of 758.4 km<sup>2</sup> of other land use types were transferred to urban built-up land, and a total of 73.02 km<sup>2</sup> of urban built-up land was transferred out (details can be seen in Appendix D and E). In this period, cropland, forest land and wetland were mainly occupied by urban expansion (details can be seen in Appendix E). The area of urban built-up land initially occupied cropland, forest land, and grassland; accounting for more than 95% of the total area of urban expansion, although it declined from 97.17% in 1980-1995 to 95.16% in 2005-2015. The stage with the rapidest urban expansion occurred in 2005-2015, whose area of urban expansion was about 1.5 times that of the past 25 years (1980-2005). From 1980 to 2015, the objects that urban built-up land transferred into were mainly cropland and wetland, whose area accounted for more than 80% of the total transferred out area. Similarly, the largest area whereby urban built-up land transferred into other land use types appeared in 2005-2015, which was 1.2 times than that of the past 25 years (1980-2005).

According to the transfer probability matrix of land use under three scenarios and the transfer rules of the model, the PLUS model was used to obtain the land use map (Figure 4) and the area of each land use type under the three scenarios in Wuhan in 2035 (Table 2). Among the three scenarios, the urban expansion area was the largest (953.32 km<sup>2</sup>) and occupied the most cropland under BS. The smallest urban expansion area (607.39 km<sup>2</sup>) was under EP, which occupied the least cropland (Table 2).

**Table 2** Land use types under the baseline scenario, cropland protection scenario, and ecological protection scenario in Wuhan in 2035.

Area(km <sup>2</sup> )	Cropland	Forest land	Grassland	River	Wetland	Urban built-up land	Rural built-up land	Unused land
2015	4,619.03	771.49	76.42	286.83	1,609.81	941.83	257.35	4,619.03
2035BS	3,578.18	733.17	41.04	283.20	1,945.01	1,740.36	243.94	3,578.18
2035CP	3,845.14	733.26	48.36	283.79	1,943.81	1,466.39	243.28	3,845.14
2035EP	3,842.53	879.36	52.71	282.97	1,916.78	1,349.00	241.22	3,842.53

By 2035, from the perspective of spatial distribution, the urban expansion of Wuhan is still expected to spread to the surrounding areas. However, compared with the EP and CP scenarios, the urban expansion of Wuhan under BS will spread more to the flat areas in the north. Under the CP scenario, the degree of urban expansion decreases, spreads less outward along secondary roads, and retains the largest amount of cropland. Under the EP scenario, urban expansion spreads the least outward along secondary roads, and some cropland in the north of Wuhan is converted to forest land.

Maintained growth of urban built-up land was observed under all three scenarios (details can be seen in Appendix D). Under the EP scenario, the area of urban built-up land is the smallest, with an estimated 1,349 km<sup>2</sup>; under BS, the area of urban built-up land is estimated to be 1,740.36 km<sup>2</sup>. Rural built-up land is expected to be the largest under BS in 2035, reaching 243.94 km<sup>2</sup>, and the least under the EP scenario, reaching 241.22 km<sup>2</sup>.

We predict that cropland will still be the largest object that urban built-up land occupies in 2035; this accounts for 89.03%, 82.57%, and 81.46% of the total area of urban expansion under BS, CP, and EP, respectively. The objects that urban built-up land transferred into were mainly cropland, wetland, and forest land, whose area accounts for approximately 93% of the total area under the three scenarios.

## 3.2 Dynamic changes of carbon storage of terrestrial ecosystems

With the rapid outward expansion of Wuhan City, its carbon storage has also undergone drastic changes (Figure 6). Initially, carbon loss was concentrated in the central area of Wuhan City from 1980 to 1995. From 1995 to 2005, the area of carbon loss expanded outward from the centre. Finally, from 2005 to 2015, carbon storage declined at the fastest rate over the past 35 years, and the area of carbon loss increased rapidly, gradually spreading from inside to outside of Wuhan city.

It is predicted that under BS, the carbon storage reduction caused by the urban expansion will be mainly concentrated in the flat area in the northwest of Wuhan and develop outward along the secondary roads by 2035. Comparatively, under the CP scenario, the carbon storage reduction caused by urban expansion will decrease and spread less along secondary roads and retain the maximum amount of cropland. Under the EP scenario, the carbon storage reduction caused by urban expansion will spread outward the least along secondary roads and part of cropland in the north of Wuhan will be converted into forest land, which generates carbon sinks.

In 1980, 1995, 2005, and 2015, the total amount of carbon storage in Wuhan's terrestrial ecosystems was respectively  $93.39 \times 10^6$  t,  $93.78 \times 10^6$  t,  $92.27 \times 10^6$  t, and  $89.96 \times 10^6$  t, and the average terrestrial ecosystem carbon density was 108.99 t/ha, 109.44 t/ha, 107.68 t/ha, and 104.98 t/ha (Figure 7). From 1980 to 2015, the carbon storage of terrestrial ecosystems in Wuhan showed a general downward trend, and the conversion of land use types contributed to the decrease of the carbon storage of terrestrial ecosystems by  $3.43 \times 10^6$  t, with an annual decline rate of 0.11%. According to the different stages of carbon storage change in Wuhan, the carbon storage dropped the most rapidly from 2005 to 2015, which decreased by  $2.31 \times 10^6$  t in 10 years, at a decline rate of 2.5%, accounting for 67.35% of the total carbon storage reduction in terrestrial ecosystems between 1980-2015.

Cropland, forest land, and wetland are the most important carbon pools in Wuhan, and these three land use types account for more than 90% of the total carbon sequestration. Among them, cropland was of the largest amount of carbon sequestration of  $49.6 \times 10^6$  t in 2015, accounting for 59.3% of the total amount of carbon sequestration in 2015.

As can be seen from the change in the trend of carbon storage of each land use type, the carbon sequestration amount of cropland and forest land showed a declining trend during the 35 years from 1980 to 2015; where the downtrend of cropland was clear, with the amount of carbon sequestration decreased by  $11.73 \times 10^6$  t at a rate of 19.13% during this period. In contrast, the decline trend of forest land is relatively flat, with the amount of carbon storage decreasing by  $0.63 \times 10^6$  t between 1980 and 2015, with a decline rate of 5.46%. Finally, carbon

sequestration in wetland and urban built-up land increased by  $5.88 \times 10^6$  t and  $3.04 \times 10^6$  t in 35 years, with growth rates of 34.15% and 267.13%, respectively. The carbon sequestration of grassland showed a trend of decline and subsequent rise; carbon storage in grassland decreased by  $0.16 \times 10^6$  t from 1980 to 2005 and then increased by  $0.11 \times 10^6$  t from 2005 to 2015; the carbon sequestration in unused land experienced increased first and then declined, and the carbon storage decreased by  $0.015 \times 10^6$  t between 1980 and 2015. The amount of carbon sequestration in rural built-up land and river remained essentially unchanged for 35 years, at  $1.1 \times 10^6$  t and zero, respectively.

From 2015 to 2035, the carbon storage of terrestrial ecosystems shows a downward trend under the three future scenarios. The carbon storage of terrestrial ecosystems under the three scenarios will reach  $86.11 \times 10^6$  t (BS),  $87.85 \times 10^6$  t (CP), and  $89.03 \times 10^6$  t (EP) by 2035. Compared to 2015, the carbon stocks will reduce by  $3.85 \times 10^6$  t (EP),  $2.11 \times 10^6$  t (CP),  $0.93 \times 10^6$  t (BS), with declining rates of 4.28%, 2.35%, and 1.04%, respectively. By 2035, the carbon sequestration capacity of the terrestrial ecosystem in Wuhan will be different under each scenario. The EP scenario shows the highest average carbon density of 103.89 t/ha, with the strongest carbon sequestration capacity. BS has the lowest carbon density, at 100.49 t/ha, and the weakest carbon sequestration capacity. In addition, from 2015 to 2035, the carbon storage in Wuhan will increase by  $3.3 \times 10^6$  t (BS),  $3.58 \times 10^6$  t (CP), and  $4.15 \times 10^6$  t (EP), while the carbon loss is  $7.2 \times 10^6$  t (BS),  $5.75 \times 10^6$  t (CP), and  $5.14 \times 10^6$  t (EP). The increase in cropland, forest land, and wetland explains the increase in carbon storage of terrestrial ecosystems. Under the three scenarios, the carbon sinks available for conversion to cropland, forest land, and wetland are  $3.26 \times 10^6$  t (BS),  $3.54 \times 10^6$  t (CP), and  $4.1 \times 10^6$  t (EP), and account for 98.82%, 98.71%, and 98.85% of the total carbon sink, respectively. Urban expansion is the leading factor resulting in carbon loss. Under the three scenarios, the carbon loss caused by urban expansion is  $6.16 \times 10^6$  t (BS),  $4.71 \times 10^6$  t (CP),  $4.06 \times 10^6$  t (EP), accounting for 85.58%, 82.01%, and 79.09% of the aggregate carbon loss, respectively.

From 2015 to 2035, the economic value of the carbon sink from the increase of carbon storage in Wuhan under BS, CP, and EP is 14.23 million USD, 15.43 million USD, and 17.88 million USD, respectively. The economic value of carbon loss is 31.02 million USD (BS), 24.76 million USD (CP), and 22.13 million USD (EP). The sum of the economic value of carbon sink and carbon loss is the final economic value of net carbon loss; in 2035, the economic value of net carbon loss under the three different scenarios will be 16.8 million USD (BS), 9.33 million USD (CP), and 4.25 million USD (EP). This means that by 2035, land use patterns in Wuhan under three future scenarios will result in a net carbon loss economic value of 19.6 USD /ha (BS), 10.89 USD /ha (CP), and 4.96 USD /ha (EP).

### **3.3 Impact of urban expansion on carbon storage of terrestrial ecosystems**

In the critical period of urbanisation, development, and transformation, Wuhan's population, economic level, cultural, and material exchanges are becoming more frequent, and urban expansion is further intensified. From 1980 to 2015, Wuhan expanded by  $758.61 \text{ km}^2$ , reducing the carbon storage of the terrestrial ecosystem by  $5.14 \times 10^6$  t. Furthermore, from 1980-2015, the area of urban built-up land respectively increased from  $256.66 \text{ km}^2$  to  $941.83 \text{ km}^2$ , the carbon storage of terrestrial ecosystems decreased from  $93.39 \times 10^6$  t to  $89.96 \times 10^6$  t, and the average carbon density decreased from 108.99 t/ha to 104.98 t/ha. The period from 2005 to 2015 was the most rapid period of urban expansion in Wuhan, and also the period in which the carbon storage of terrestrial

ecosystems declined the most rapidly. During this period, the urban expansion of Wuhan was 453.3 km<sup>2</sup>, which led to a decrease of 3.02×10<sup>6</sup> t in carbon storage. During 1980–1995, 1995–2005, and 2005–2015, the influence of urban expansion on the carbon reserve in Wuhan gradually increased, reducing carbon storage by 0.83×10<sup>6</sup> t, 1.29×10<sup>6</sup> t and 3.02×10<sup>6</sup> t, which accounted for 49.7%, 60.85%, and 74.02% of the total carbon loss, respectively.

**Table 3** Effect of urban expansion on carbon storage in terrestrial ecosystems in Wuhan.

	1980	1995	2005	2015	2015	2015
	-1995	-2005	-2015	-2035BS	-2035CP	-2035EP
Urban expansion/km <sup>2</sup>	124.93	180.38	453.3	953.32	705.69	607.39
Carbon loss due to urban expansion/10 <sup>6</sup> t	-0.83	-1.29	-3.02	-6.15	-4.7	-4.05
Total carbon loss/10 <sup>6</sup> t	-1.67	-2.12	-4.08	-7.2	-5.75	-5.14
Net carbon loss/10 <sup>6</sup> t	0.34	-1.55	-2.26	-3.9	-2.17	-0.99
Economic value of carbon loss due to urban expansion/million USD	-4.23	-8.05	-18.81	-26.5	-20.26	-17.45
Economic value of total carbon loss/million USD	-8.55	-13.2	-23.83	-31.02	-24.76	-22.13
Economic value of net carbon loss/million USD	1.73	-9.65	-14.05	-16.79	-9.33	-4.25

From 2015 to 2035, compared with the other two scenarios, the area of urban expansion in the study area is expected to be the largest under BS, reaching 953.32 km<sup>2</sup> and causing a maximum carbon loss of 6.15×10<sup>6</sup> t and a maximum economic loss of 26.5 million USD. Among them, urban expansion at the expense of cropland caused a carbon storage loss of 5.35×10<sup>6</sup> t and an economic loss of 23.06 million USD, accounting for 87.01% of the carbon loss and economic damage led by urban sprawl. In this scenario, the total carbon loss is 7.2×10<sup>6</sup> t, 85.42% and is caused by urban expansion. The conversion of cropland to wetland is the main source of the carbon sink in this scenario, with a converted area of 383.22 km<sup>2</sup>, bringing a carbon sink of 1.38×10<sup>6</sup> t, and generating an economic value of 5.96 million USD.

It is estimated that Wuhan's urban expansion area will reach 705.69 km<sup>2</sup> under the CP scenario by 2035, causing a carbon loss of 4.7×10<sup>6</sup> t, and an economic loss of 20.26 million USD. Among them, urban expansion at the expense of cropland will cause a carbon storage loss of 3.67×10<sup>6</sup> t and an economic loss of 15.83 million USD, accounting for 78.13% of the carbon loss and economic damage led by urban sprawl. In this scenario, the total carbon loss is 5.75×10<sup>6</sup> t, with 81.74% of the carbon loss caused by urban expansion. The conversion of cropland to wetland is the main source of carbon sink under this scenario, with a converted area of 416.37 km<sup>2</sup>, bringing 1.5×10<sup>6</sup> t of carbon sink and generating economic value of 6.47 million USD.

The area of urban expansion in Wuhan will reach a minimum of 607.39 km<sup>2</sup> under the EP scenario in 2035, resulting in a corresponding minimum carbon loss of 4.05×10<sup>6</sup> t, and a minimum economic loss of 17.45 million USD. Among them, urban expansion at the expense of cropland will cause a loss of 3.12×10<sup>6</sup> t of carbon storage and an economic loss of 13.44 million USD, accounting for 77.01% of the carbon loss and economic damage led

by urban sprawl. In this scenario, the total carbon loss is  $5.14 \times 10^6$  t, of which 78.79% of carbon loss is caused by urban expansion. The conversion of cropland to wetland and forest land is the main source of carbon sink under this scenario, in which the converted area of cropland to wetland is  $355.36 \text{ km}^2$ , bringing  $1.28 \times 10^6$  t of carbon sink, and generating economic value of 5.52 million USD, while a total of  $219.59 \text{ km}^2$  of cropland will be converted to forest land, resulting in a  $0.76 \times 10^6$  t carbon sink and an economic value of 3.26 million USD.

Carbon storage in regional ecosystems is largely affected by urban expansion (An and Zhang, 2016; Yan et al., 2017), and urban planning is the blueprint of urban development in a given period, affecting the speed and direction of urban expansion. Therefore, it is crucial to study the space-time mode of urban expansion under different policies. Based on the historical development model and cropland protection and ecological protection policies, this study projected three different scenarios to discuss the impact of different urban development strategies on carbon storage terrestrial ecosystems. The results show that under the historical development scenario (BS), the carbon storage loss led by urban sprawl between 2015 and 2035 is expected to be 1.42 times that during 1990–2015, but the corresponding economic loss is expected to be only slightly lower. The net carbon loss in Wuhan between 2015 and 2035 only increased by 2.36% compared with the period from 1990–2015, which may be due to the national development of the environmental protection industry and the implementation of environmental protection policies. Under the EP scenario, the enhanced protection of ecological land limits the conversion of ecological land to urban built-up land. Therefore, the carbon storage loss caused by urban expansion under the EP scenario is the lowest. The net carbon loss under the EP scenario between 2015 and 2035 is approximately 1/4 of that in 1990–2015, and the corresponding economic value loss is 17.93% of that in 1990–2015. Under the historical development scenario (BS), the net carbon loss from 2015 to 2035 is projected to increase compared with that from 1990 to 2015, while under the CP and EP scenarios, the net carbon loss from 2015 to 2035 is moderate compared with that from 1990 to 2015. This shows that cropland and ecological protection policies can both have a significant effect for limiting urban expansion and reducing carbon loss, which is conducive to slowing down greenhouse gas emissions and global warming.

## 4. Discussion

### 4.1 Associated factors on carbon storage within urban expansion

The PLUS model constructs a new data mining frame for discerning land use change patterns to help reveal potential driving factors and their different contributions. Specifically, the LEAS module in the PLUS model extracts the expansion of various types of land between the two phases of land use changes and then samples from the increased parts. Finally, the random forest algorithm is utilised to pair each type of land use expansion and driving force to explore the factors to obtain the development probability of various types of land use and the contribution of driving factors to the expansion of various types of land use during this period.

**Table 4** Land use type in the 1-km buffer zone of the secondary road in 2005 and 2015.

Area(km <sup>2</sup> )	Cropland	Forest land	Grassland	River	Wetland	Urban built-up land	Rural built-up land	Unused land
2005	1747.61 (61.11%)	132.49 (4.63%)	26.5 (0.93%)	77.47 (2.71%)	340.06 (11.89%)	435.33 (15.22%)	93.33 (3.26%)	6.95 (0.24%)
2015	1502.37 (52.54%)	126.09 (4.41%)	33.76 (1.18%)	76.15 (2.66%)	323.18 (11.30%)	705.47 (24.67%)	88.40 (3.09%)	3.87 (0.14%)

Figure 10 shows the ranking of the contribution of the 15 selected driving factors to the expansion of urban built-up land and rural built-up land. The primary driving factors of rural built-up land were the average annual temperature and the distance to secondary roads and highways. The newly added rural built-up land had a certain correlation with temperature, and it was often distributed in relatively high-temperature areas. The main driving factors of urban built-up land were terrain, distance to secondary roads and tertiary roads, in which the distance to secondary roads was the most weighted factor. The newly added urban built-up land of Wuhan from 2005 to 2010 that was used to verify the accuracy of the model was concentrated around the secondary roads; i.e. urban expansion tended to appear around the secondary roads. Based on the 1 km buffer analysis of the secondary road (Table 4), ecological land, such as cropland, forest land, and wetland, was the major land use type excluding urban built-up land in the 1-km buffer zone of the secondary road in 2005. Thus, we can conclude that when urban built-up land expands outward along secondary roads, most of the occupied land is ecological land which is of high carbon density, causing the carbon loss district centred around secondary roads. Similarly, in 2015, ecological land was the dominant land in the 1-km buffer zone of the secondary road, which may suggest that urban expansion will be at the cost of the ecological land in 2035.

## 4.2 Practical implications

Since the reform and opening-up, China's economic growth has accelerated, cities have expanded rapidly, and environmental problems have emerged. Environmental protection has obeyed and served economic development. Ecosystem service decline accompanies environmental degradation; however, ecosystem services play a pivotal part in human well-being. In particular, carbon storage is closely related to global warming and extreme climate issues (Goh et al., 2017; Li et al., 2021). After 2012, China's economic development has entered a new normal, and environmental protection has received unprecedented attention and gradually been integrated into economic development. In 2020, China proposed the strategic goal of achieving a carbon peak by 2030 and carbon neutrality by 2060 (Dong et al., 2021). Presently, more than 110 countries worldwide have successively committed to carbon neutrality by the mid-21st century.

Wuhan City proposed *Wuhan City Carbon Emission Peak Action Plan (2017-2022)* in 2017, which stipulates that Wuhan City's carbon emissions will peak by 2022 (Rocky Mountain Institute, 2018). The plan proposes six paths to achieve carbon peaks: one is to reduce urban carbon emissions by optimising the urban ecological layout, implementing ecological environmental protection restoration projects, and increasing urban carbon sinks. This study set up a variety of scenarios based on different policies and conducted scenario comparison to analyse the impact of urban expansion on carbon storage and the corresponding changes in economic value. This can provide data support for optimising the urban ecological layout for government departments, increasing urban

carbon sinks, and achieving urban sustainability. Our research proves the feasibility of designing scenarios and simulates future changes in urban land use patterns and carbon storage from the socioeconomic, environmental factors of urban expansion and different urban development policies. Evidently, more factors should be considered to improve the method when setting up scenarios, such that the city can strike a balance between social and economic development and ecosystem protection to achieve sustainable development. Specifically, more consideration should be given to the ecological land around the secondary roads if decision-makers want to hold back the downward trend of carbon storage due to Wuhan's urbanisation, which tends to be at the cost of ecological land around the secondary roads.

### **4.3 Limitations and future directions**

Based on the InVEST model, this study used Wuhan's land use data and carbon density data to calculate the carbon storage of the study area, which was different from the actual carbon storage owing to the effect of environmental water and heat conditions, human activities, vegetation growth, etc. (Ke and Tang, 2019). Since the InVEST model estimates carbon storage of land use, its results are mostly credible for different land use types; and even for the same land use type, there are significant differences in carbon density (Rijal, 2019). Moreover, the carbon storage module of the InVEST model simplifies the principle of the carbon cycle process to facilitate the calculation of carbon storage (Deng et al., 2020). The model assumes that no land use type in the landscape will gain or lose carbon over time. Therefore, the carbon storage of terrestrial ecosystems in the entire study area will only change with the transformations of each land use type in the area during the study period (Liu et al., 2019). In fact, many regions are gradually transforming from past land use patterns, or are experiencing natural succession, and carbon storage is increasing as a result (Sun et al., 2018). Due to factors like human activities and environmental changes, carbon density will change with time (Zhu et al., 2019), and regional ecosystem carbon storage will convert, owing to changes in land use types and shifts in carbon density at different times.

Moreover, the carbon density data required for the calculations in this study were all sourced from previous related studies without field verification and testing, which naturally caused a certain error in the calculation of carbon storage. In future research, the accuracy of the carbon density should be validated by obtaining measured data through field investigations. Continuous monitoring of the selected sample plots should also be conducted in the study area over a period of time to allow for the spatial heterogeneity of land use types and the impact of vegetation age structure on carbon density to be updated and supplemented in time (Zhu et al., 2019), making the evaluation results of the InVEST model more accurate.

When using the PLUS and Markov model to project the amount and spatial distribution of land use in future scenarios, the relevant policy documents referred to cannot be directly converted into the constraints and rules required by the model, and they are not time-effective. Furthermore, the three future land use scenarios described in this study cannot represent all possible land use conditions. In the future, the parameters and conversion rules of the PLUS model should be adjusted and combined with local development policies. The development process of the natural and social systems of the study area should be heeded to comprehensively set up a land use development scenario that is closer to reality and in line with policy guidance to meet the needs of government departments when formulating land use policies (Liang et al., 2018; Zheng et al., 2019).

## **5. Conclusion**

Based on the PLUS model, this study firstly simulated the land use status of Wuhan in 2035 under different scenarios and analysed the changes of the urban expansion pattern from 1980 to 2015 and from 2015 to 2035 from spatial and temporal perspectives. Then, the InVEST model was used to evaluate the impact of land use change caused by urban sprawl on carbon storage change in Wuhan between 1980 and 2015 and from 2015 to 2035. Finally, the social cost of carbon was applied to calculate the economic loss caused by carbon storage reduction under the influence of urban expansion. The following conclusions were drawn:

(1) There was rapid urban expansion in Wuhan from 1980 to 2015. The urban sprawl was primarily concentrated in the central plain district and tended to spread from the centre to the periphery, mainly extending to the south. The period from 2005 to 2015 exhibited the most rapid expansion stage, and the cropland was the main type occupied by urban expansion. According to the LEAS module of the PLUS model, among the 15 selected driving factors of the social and economic environment, secondary roads had the greatest impact on urban expansion, and most of the new urban built-up land centred around secondary roads.

(2) During 1980–2015, the carbon storage in Wuhan City showed an overall downward trend, with the most rapid decline occurring between 2005 and 2015. It is expected that the carbon storage in Wuhan will further decrease by 2035, but the relevant protection policies implemented by government departments will slow this trend.

(3) Wuhan is experiencing rapid urban expansion, which greatly influences carbon storage in Wuhan. From 1980 to 2015, the carbon loss caused by urban expansion gradually increased, and the ratio of carbon loss to the total carbon loss under the influence of urban expansion gradually increased. It is expected that this proportion will increase further by 2035, wherein Wuhan's net carbon loss under BS will increase, while the net carbon loss under CP and EP scenario will be greatly reduced. It suggests that implementing farmland protection policies and ecological protection policies can alleviate the impact of urban expansion on carbon storage to a certain extent and decrease the resulting economic loss under the effect of urban sprawl.

The coupled use of the PLUS and InVEST model in this study can quickly and effectively assess the potential impact of urban expansion on regional carbon storage and provide a reference for future spatial planning of Wuhan, thereby promoting regional sustainable development. Additionally, for different urban development policies, the calculation and evaluation of carbon storage changes and their corresponding economic value based on these models can help to analyse the pros and cons of different policies. However, carbon storage is only one of many ecosystem services. When analysing policy feasibility, the value of multiple ecosystem services should also be scrutinised.

## **Declarations**

### **Ethical approval**

All ethical practices have been followed in relation to the data analysis, writing and publication of this research article.

### **Consent to Participate**

Not applicable.

### **Consent to Publish**



Not applicable.

## Authors Contributions

Jie Zeng and Zhuo Wang: Methodology, Writing - original draft, Resources. Jie Zeng and Wanxu Chen: Conceptualization, Supervision. Jie Zeng and Wanxu Chen: Writing - review & editing. Zhuo Wang: Software, Data curation.

## Funding

The research is sponsored in part by grants from the Natural Science Foundation of China (Grant No. 42001187, NO.41701629 and NO.42001231). The project was also supported by State Key Laboratory of Earth Surface Processes and Resource Ecology (2021-KF-03).

## Competing Interests

The authors declare that they have no known competing financial interests or personal relationships that could have appeared to influence the work reported in this paper.

## Availability of data and materials

The data used in the current study will be available from the corresponding author upon request via e-mail.

## Acknowledgements

The authors are very grateful to the many people involved in the data collection for this article and review of this work.

## References

1. An, Y., Zhang, Q., 2016. Impact of rapid urbanization on temporal and spatial variation of Shanghai vegetation and soil carbon storage. *Environ. Sci. Manage.* 41 (08), 152-155+170.
2. Baumann, M., Gasparri, N., Piquer-Rodríguez, M., Gavier-Pizarro, G., Griffiths, P., Hostert, P., Kuemmerle, T., 2016. Carbon emissions from agricultural expansion and intensification in the Chaco. *Glob. Change Biol.* 23.
3. Chen, B., Liao, T., Zhang, L., 2020. Simulation of land use situation and ecological value assessment in Wanzhou district under the constraints of ecological red line. *Res. Soil Water Conserv.* 27 (05), 349-357+364.
4. Chen, W., Chi, G., Li, J., 2020. Ecosystem services and their driving forces in the Middle Reaches of the Yangtze River Urban Agglomerations, China. *Int. J. Environ. Res. Public Health* 17, 3717.
5. Chen, W., Zhao, H., Li, J., Zhu, L., Wang, Z., Zeng, J., 2019. Land use transitions and the associated impacts on ecosystem services in the Middle Reaches of the Yangtze River Economic Belt in China based on the geoinformatic Tupu method. *Sci. Total Environ.* 701, 134690.
6. Chen, Y.M., Li, X., Liu, X.P., Ai, B., 2014. Modeling urban land-use dynamics in a fast developing city using the modified logistic cellular automaton with a patch-based simulation strategy. *Int. J. Geogr. Inf. Sci.* 28 (2), 234-255.
7. Chuai, X., Huang, X., Zheng, Z., Zhang, M., Liao, Q., LAI, L., Lu, J., 2011. Land use change and its influence on carbon storage of terrestrial ecosystems in Jiangsu Province. *Resour. Sci.* 33 (10), 1932-1939.

8. Cohen, J., 1960. A coefficient of agreement for nominal scales. *Educ. Psychol. Meas.* 20 (1), 37-46.
9. Deng, Y., Yao, S., Hou, M., Zhang, T., Lu, Y., Gong, Z., Wang, Y., 2020. Assessing the effects of the green for grain program on ecosystem carbon storage service by linking the InVEST and FLUS models: a case study of Zichang county in hilly and gully region of Loess Plateau. *J. Nat. Resour.* 35 (4), 826-844.
10. Dong, L., Miao, G.Y., Wen, W.G., 2021. China's carbon neutrality policy: Objectives, impacts and paths. *East Asian Policy* 13 (01), 5-18.
11. Fang, J., Yu, G., Ren, X., Liu, G., Zhao, X., 2015. Carbon sequestration in China's terrestrial ecosystems under climate change – Progress on ecosystem carbon sequestration from the CAS strategic priority research program. *Bull. Chin. Acad. Sci.* 30 (06), 848-857+875.
12. Feng, Y., Chen, S., Tong, X., Lei, Z., Gao, C., Wang, J., 2020. Modeling changes in China's 2000–2030 carbon stock caused by land use change. *J. Clean Prod.* 252, 119659.
13. Gao, J., Wang, L., 2019. Embedding spatiotemporal changes in carbon storage into urban agglomeration ecosystem management – A case study of the Yangtze River Delta, China. *J. Clean Prod.* 237, 117764.
14. Goh, C.S., Wicke, B., Potter, L., Faaij, A., Zoomers, A., Junginger, M., 2017. Exploring under-utilised low carbon land resources from multiple perspectives: Case studies on regencies in Kalimantan. *Land Use Pol.* 60, 150-168.
15. He, C., Zhang, D., Huang, Q., Zhao, Y., 2016. Assessing the potential impacts of urban expansion on regional carbon storage by linking the LUSD-urban and InVEST models. *Environ. Modell. Software* 75, 44-58.
16. He, X., 2004. An empirical analysis of urbanization process in Wuhan city. *J. Zhongnan Univ. Economics Law* 2004 (05), 56-60+142-143.
17. Houghton, R., House, J., Pongratz, J., Werf, G., Defries, R., Hansen, M., Le Quéré, C., Ramankutty, N., 2012. Chapter G2 Carbon emissions from land use and land-cover change. *Biogeosciences* 9, 5125-5142.
18. Ke, X.L., Tang, L.P., 2019. Impact of cascading processes of urban expansion and cropland reclamation on the ecosystem of a carbon storage service in Hubei Province, China. *Acta Ecol. Sin.* 39 (02), 672-683.
19. Lahiji, R.N., Dinan, N.M., Liaghati, H., Ghaffarzadeh, H., Vafaeinejad, A., 2020. Scenario-based estimation of catchment carbon storage: linking multi-objective land allocation with InVEST model in a mixed agriculture-forest landscape. *Front. Earth Sci.* 14 (3), 637-646.
20. Li, J., Gong, J., Guldmann, J.-M., Li, S., Zhu, J., 2020. Carbon dynamics in the Northeastern Qinghai–Tibetan Plateau from 1990 to 2030 using landsat land use/cover change data. *Remote Sens.* 12 (3), 528.
21. Li, J., Zhang, C., Zhu, S., 2021. Relative contributions of climate and land-use change to ecosystem services in arid inland basins. *J. Clean Prod.* 298, 126844.
22. Li, W., Lan, Z., Chen, D., Zheng, Z., 2020. Multi-scenario simulation of land use and its spatial-temporal response to ecological risk in Guangzhou city. *Bull. Soil Water Conserv.* 40 (04), 204-210+227+202.
23. Liang, X., Liu, X., Li, D., Zhao, H., Chen, G., 2018. Urban growth simulation by incorporating planning policies into a CA-based future land-use simulation model. *Int. J. Geogr. Inf. Sci.* 32 (11-12), 2294-2316.
24. Liang, X., Guan, Q., Clarke, K.C., Liu, S., Wang, B., Yao, Y., 2021. Understanding the drivers of sustainable land expansion using a patch-generating land use simulation (PLUS) model: A case study in Wuhan, China. *Comput. Environ. Urban Syst.* 85.
25. Liang, Y.J., Hashimoto, S., Liu, L.J., 2021. Integrated assessment of land-use/land-cover dynamics on carbon storage services in the Loess Plateau of China from 1995 to 2050. *Ecol. Indic.* 120, 14.

26. Liu, J.Y., Kuang, W., Zhang, Z., Xu, X., Qin, Y.W., Ning, J., Zhou, W., Zhang, S., Li, R., Yan, C., Wu, S.X., History, X., Jiang, S., Yu, D., Pan, X., Chi, W.F., 2014. Spatiotemporal characteristics, patterns, and causes of land-use changes in China since the late 1980s. *J. Geogr. Sci.* 24 (02), 195-210.
27. Liu, X., Liang, X., Li, X., Xu, X., Ou, J., Chen, Y., Li, S., Wang, S., Pei, F., 2017. A future land use simulation model (FLUS) for simulating multiple land use scenarios by coupling human and natural effects. *Landscape Urban Plann.* 168. 94-116.
28. Liu, X., Wang, S., Wu, P., Feng, K., Hubacek, K., Li, X., Sun, L., 2019. Impacts of urban expansion on terrestrial carbon storage in China. *Environ. Sci. Technol.* 53 (12), 6834-6844.
29. Lu, R., Huang, H.K., Left, T., Xiao, S., Zhao, X., Zhang, X., 2009. Land use scenarios simulation based on CLUE-S and Markov composite model: A case study of Taihu Lake Rim in Jiangsu Province. *Sci. Geogr. Sin.* 29 (04), 577-581.
30. Lyu, R., Mi, L., Zhang, J., Xu, M., Li, J., 2019. Modeling the effects of urban expansion on regional carbon storage by coupling SLEUTH-3r model and InVEST model. *Ecol. Res.* 34.
31. Maanan, M., Karim, M., Kacem, H.A., Ajrhoug, S., Rueff, H., Snoussi, M., Rhinane, H., 2019. Modelling the potential impacts of land use/cover change on terrestrial carbon stocks in north-west Morocco. *Int. J. Sustain. Dev. World Ecol.* 26 (6), 560-570.
32. Meentemeyer, R.K., Tang, W., Dorning, M.A., Vogler, J.B., Shoemaker, D.A., 2013. FUTURES: Multilevel simulations of emerging urban–rural landscape structure using a stochastic patch-growing algorithm. *Ann. Assoc. Am. Geogr.* 103 (4).
33. Pontius, R.G., Boersma, W., Castella, J.C., Clarke, K., de Nijs, T., Dietzel, C., Duan, Z., Fotsing, E., Goldstein, N., Kok, K., Koomen, E., Lippitt, C.D., McConnell, W., Sood, A.M., Pijanowski, B., Pithadia, S., Sweeney, S., Trung, T.N., Veldkamp, A.T., Verburg, P.H., 2008. Comparing the input, output, and validation maps for several models of land change. *Ann. Reg. Sci.* 42 (1), 11-37.
34. Pontius, R.G., Millones, M., 2011. Death to Kappa: birth of quantity disagreement and allocation disagreement for accuracy assessment. *Int. J. Remote Sens.* 32 (15), 4407-4429.
35. Rijal, S., 2019. Effects of land use and land cover change on ecosystem services in the Koshi River Basin, Eastern Nepal. *Ecosyst. Serv.* 38.
36. Rocky Mountain Institute, 2018. Analyzing carbon emissions peaking pathway of the industrial sector in Wuhan. America.
37. Sadat, M., Zoghi, M., Malekmohammadi, B., 2020. Spatiotemporal modeling of urban land cover changes and carbon storage ecosystem services: case study in Qaem Shahr County, Iran. *Environ. Dev. Sustain.* 22 (8), 8135-8158.
38. Sallustio, L., Quatrini, V., Geneletti, D., Corona, P., Marchetti, M., 2015. Assessing land take by urban development and its impact on carbon storage: Findings from two case studies in Italy. *Environ. Impact Assess. Rev.* 54, 80-90.
39. Sharp, R., Tallis, H. T., Ricketts, T., Guerry, A. D., Wood, S. A., Chapin-Kramer, R., N., E., Ennaanay, D., Wolny, S., Olwero, N., Vigerstol, K., Pennington, D., M., G., Aukema, J., Foster, J., Forrest, J., Cameron, D., Arkema, K., Lonsdorf, E., Kennedy, C., Verutes, G., Kim, C. K., Guannel, G., Papenfus, M., Toft, J., Marsik, M., Bernhardt, J., Griffin, R., Gowinski, K., Chaumont, N., Perelman, A., Lacayo, M. Mandle, L., Hamel, P., Vogl, A. L., Rogers, L., and Bierbower, W., 2015. InVEST 3.2.0 user's guide. The Natural Capital Project, Stanford University, University of Minnesota, The Nature Conservancy, and World Wildlife Fund.

40. Sohl, T.L., Claggett, P.R., 2013. Clarity versus complexity: Land-use modeling as a practical tool for decision-makers. *J. Environ. Manage.* 129 (nov.15), 235-243.
41. Stuver, M., 1978. Atmospheric Carbon Dioxide and Carbon Reservoir Changes. *Sci.* 199, 253-258.
42. Sun, X., Lu, Z., Li, F., Crittenden, J., 2018. Analyzing spatio-temporal changes and trade-offs to support the supply of multiple ecosystem services in Beijing, China. *Ecol. Indic.* 94 (nov.), 117-129.
43. Tang, R., Peng, K., 2018. Impact of land use change on regional land carbon storage: A review. *Jiangsu Agric. Sci.* 46 (19), 5-11.
44. Tian, L., Ye, Q., Zhen, Z., 2019. A new assessment model of social cost of carbon and its situation analysis in China. *J. Clean Prod.* 211, 1434-1443.
45. Wang, J.Z., Zhang, Q., Gou, T.J., Mo, J.B., Wang, Z.F., Gao, M., 2018. Spatial-temporal changes of urban areas and terrestrial carbon storage in the Three Gorges Reservoir in China. *Ecol. Indic.* 95, 343-352.
46. Wang, X., Ma, B., Li, D., Chen, K., Yao, H.S., 2020. Multi-scenario simulation and prediction of ecological space in Hubei Province based on FLUS model. *J. Nat. Resour.* 35 (01), 230-242.
47. Wu, P., Liu, X., Li, X., Chen, Y., 2016. Evaluation of the impact of urban expansion on the carbon storage of terrestrial ecosystem based on InVEST model and Cellular Automata in Guangdong Province, China. *Geogr. Geo-Inf. Sci.* 32(05), 22-28+36+22.
48. Yan, J.T., Wang, J., Lu, S., Zeng, H., 2017. Impacts of rapid urbanization on carbon dynamics of urban ecosystems in Shenzhen. *Ecol. Environ. Sci.* 26(04), 553-560.
49. Yang, J., Gong, J., Tang, W., Liu, C., 2020. Patch-based cellular automata model of urban growth simulation: Integrating feedback between quantitative composition and spatial configuration. *Comput. Environ. Urban Syst.* 79, 101402.
50. Yang, H., Huang, J., Liu, D., 2020. Linking climate change and socioeconomic development to urban land use simulation: Analysis of their concurrent effects on carbon storage. *Appl. Geogr.* 115, 102135.
51. Zhao, Z., Liu, G., Mou, N., Xie, Y., Xu, Z., Li, Y., 2018. Assessment of Carbon Storage and Its Influencing Factors in Qinghai-Tibet Plateau. *Sustain.* 10, 1864.
52. Zeng, J., Chen, T., Yao, X., Chen, W., 2020. Do protected areas improve ecosystem services? A case study of Hoh Xil Nature Reserve in Qinghai-Tibetan Plateau. *Remote Sens.* 12(3).
53. Zheng, H., Wang, L., Peng, W., Zhang, C., Daily, G.C., 2019. Realizing the values of natural capital for inclusive, sustainable development: Informing China's new ecological development strategy. *Proc. Natl. Acad. Sci.* 116(17), 8623-8628.
54. Zhu, W., Zhang, J., Cui, Y., Zheng, H., Zhu, L., 2019. Assessment of territorial ecosystem carbon storage based on land use change scenario: A case study in Qihe River Basin. *Acta Geogr. Sin.* 74(03), 446-459.

## Figures

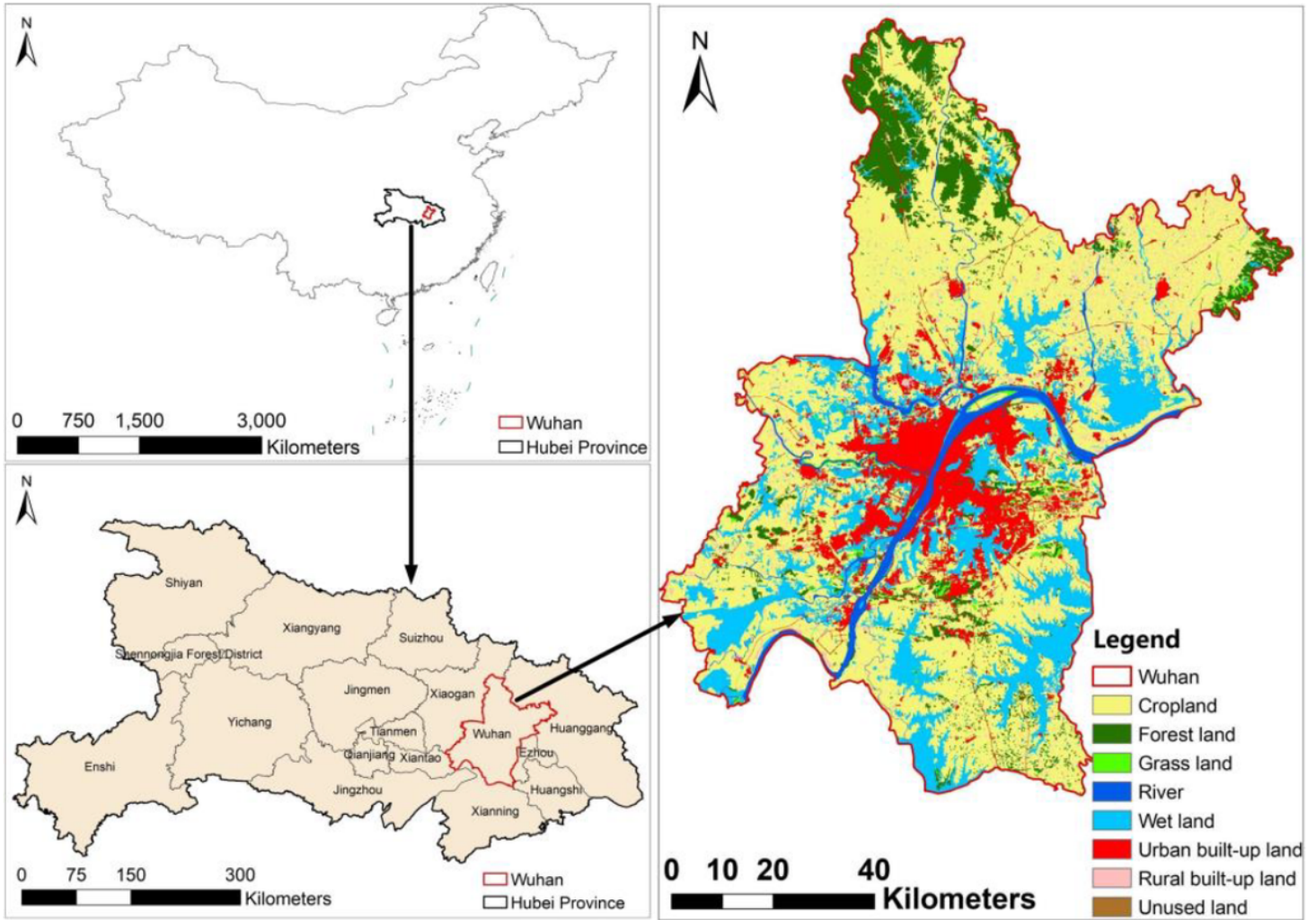
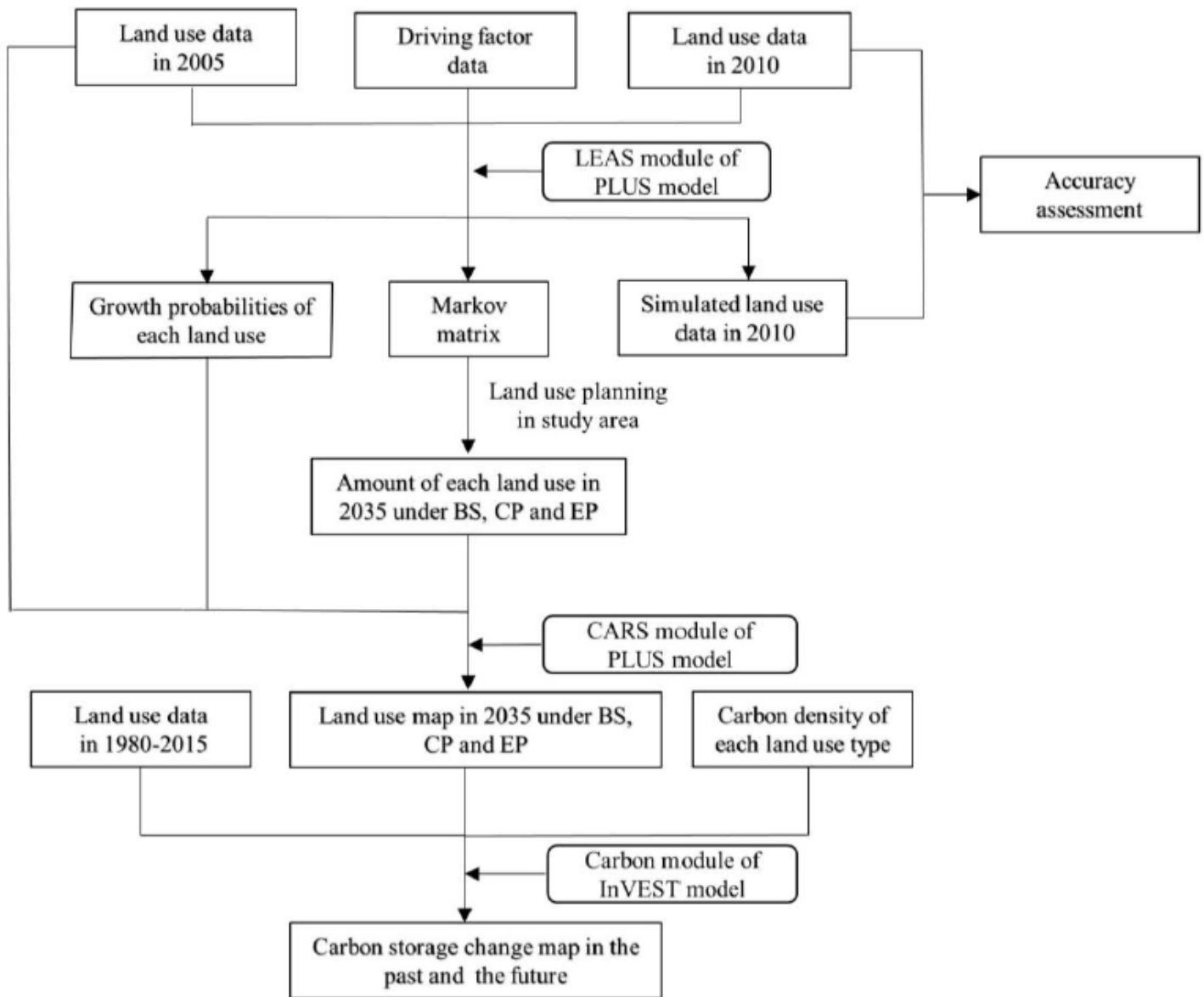


Figure 1

Location of Wuhan in China.



**Figure 2**

Overall experimental process in this study

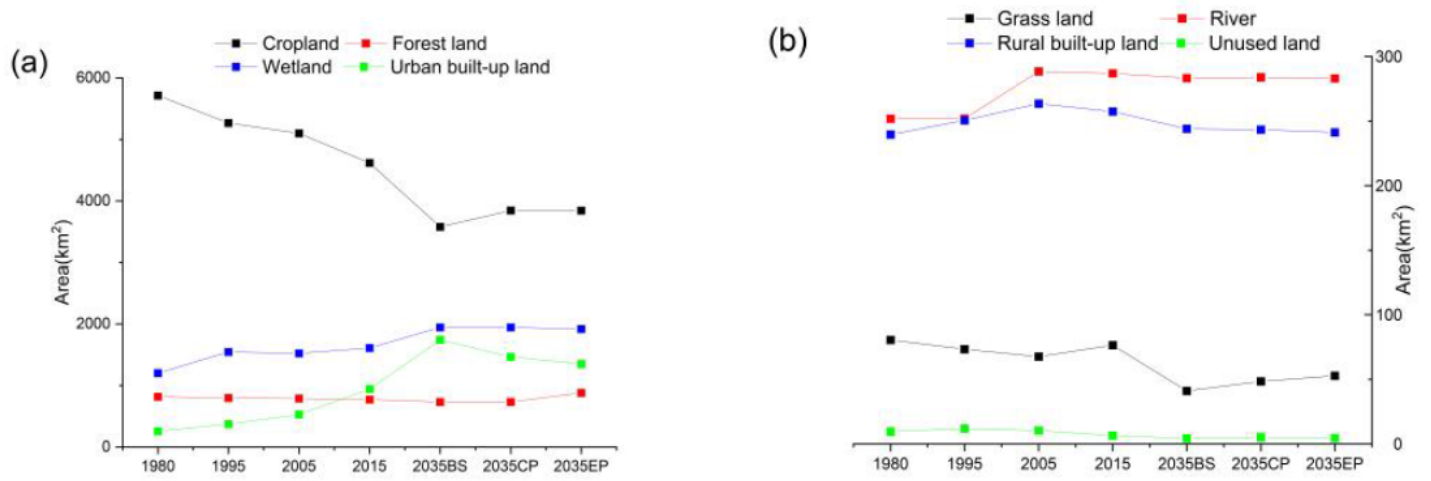
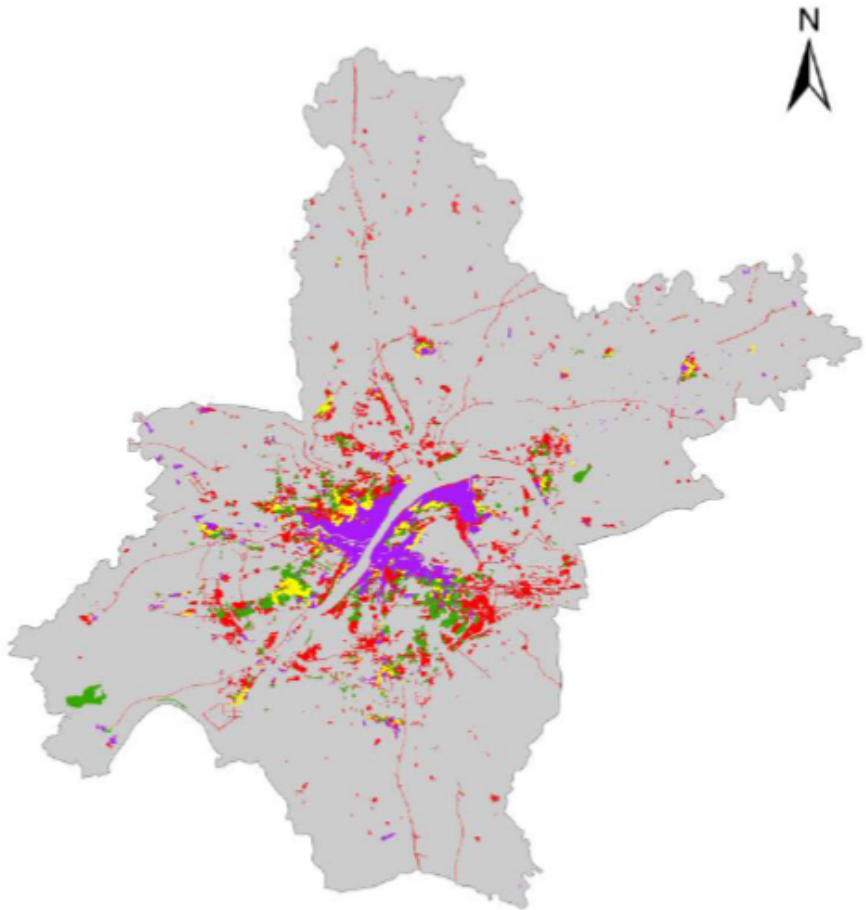



**Figure 3**

Land use change from 1980 to 2035 in Wuhan. (a) Area changes of cropland, forest land, wetland, urban built-up land; (b) area changes of grass land, river, rural built-up land and unused land.



**Legend**

- Urban built-up land in 1980
- Urban expansion in 1980-1995
- Urban expansion in 1995-2005
- Urban expansion in 2005-2015
- No change or other types of growth

 Kilometers  
0 5 10 20 30 40

**Figure 4**

Urban expansion of Wuhan from 1980 to 2015.



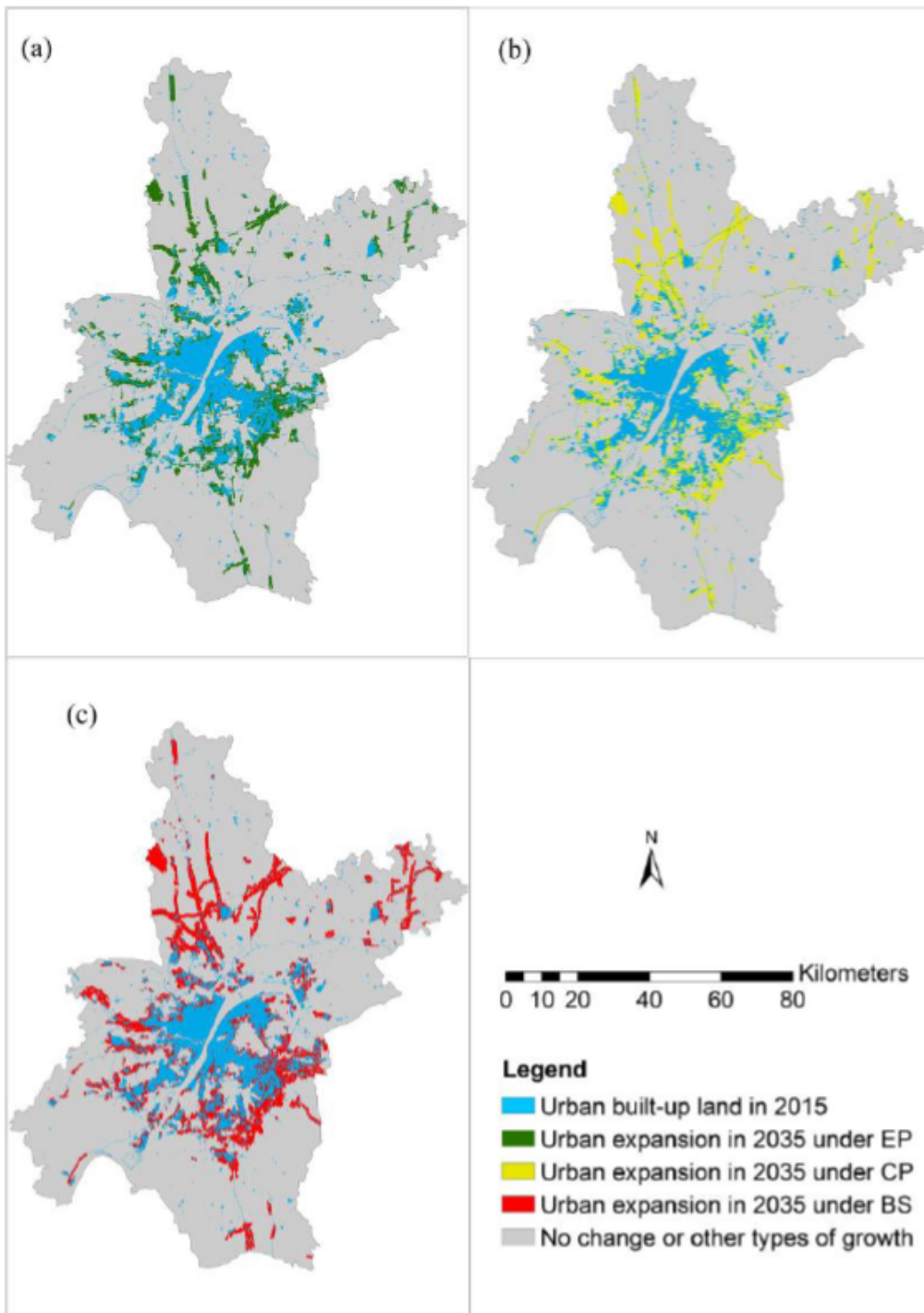


**Figure 5**

Urban expansion of Wuhan from 2015 to 2035. (a) Projected urban expansion from 2015 to 2035 under EP; (b) Projected urban expansion from 2015 to 2035 under CP; (c) Projected urban expansion from 2015 to 2035 under BS.

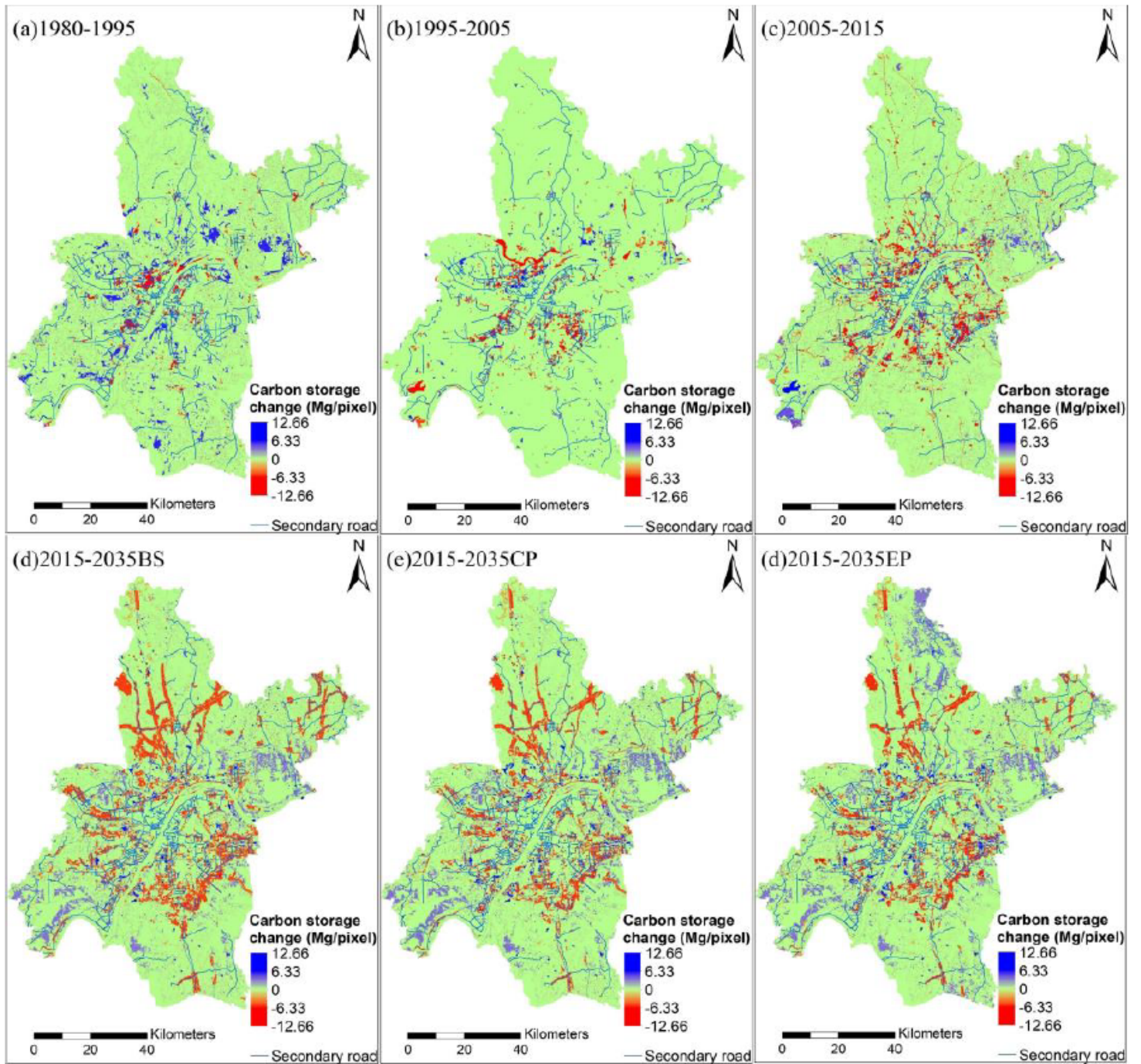


**Figure 6**

Spatial change in carbon storage in Wuhan City from 1980 to 2035. (a) 1980-1995; (b) 1995-2005; (c) 2005-2015; (d) 2015-2035 under BS; (e) 2015-2035 under CP; (f) 2015-2035 under EP.

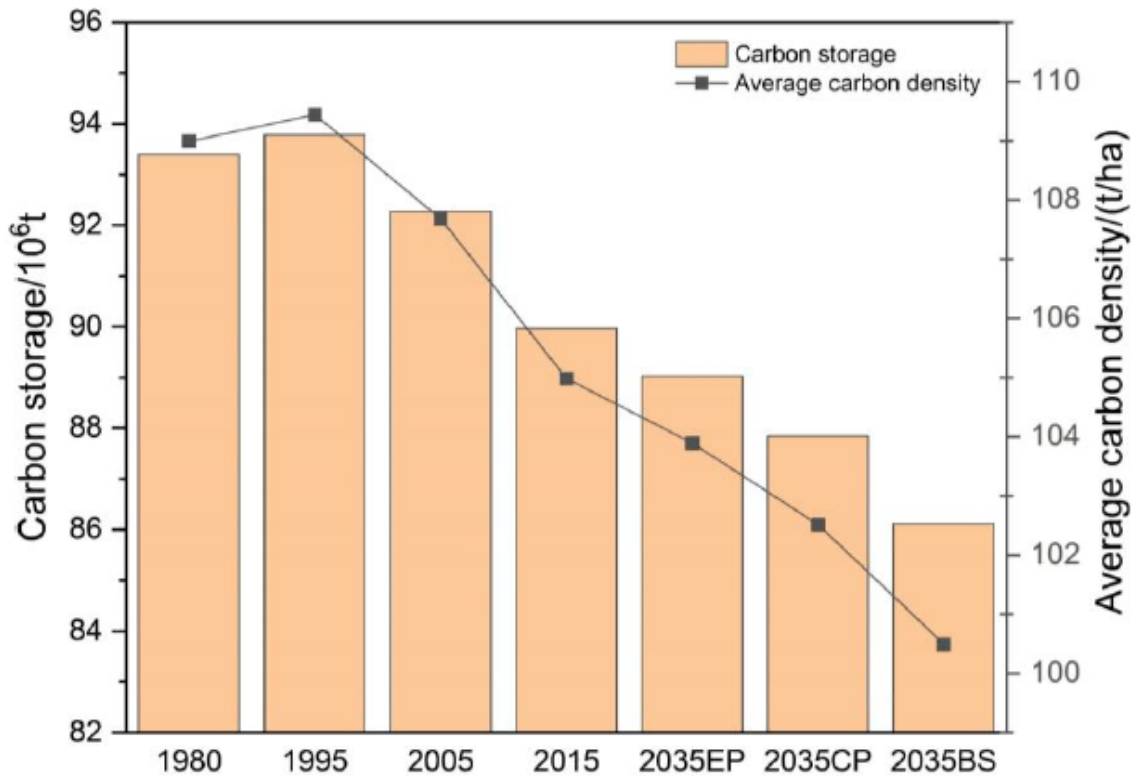


**Figure 7**

Changes in carbon storage and average carbon density in Wuhan from 1980 to 2035.

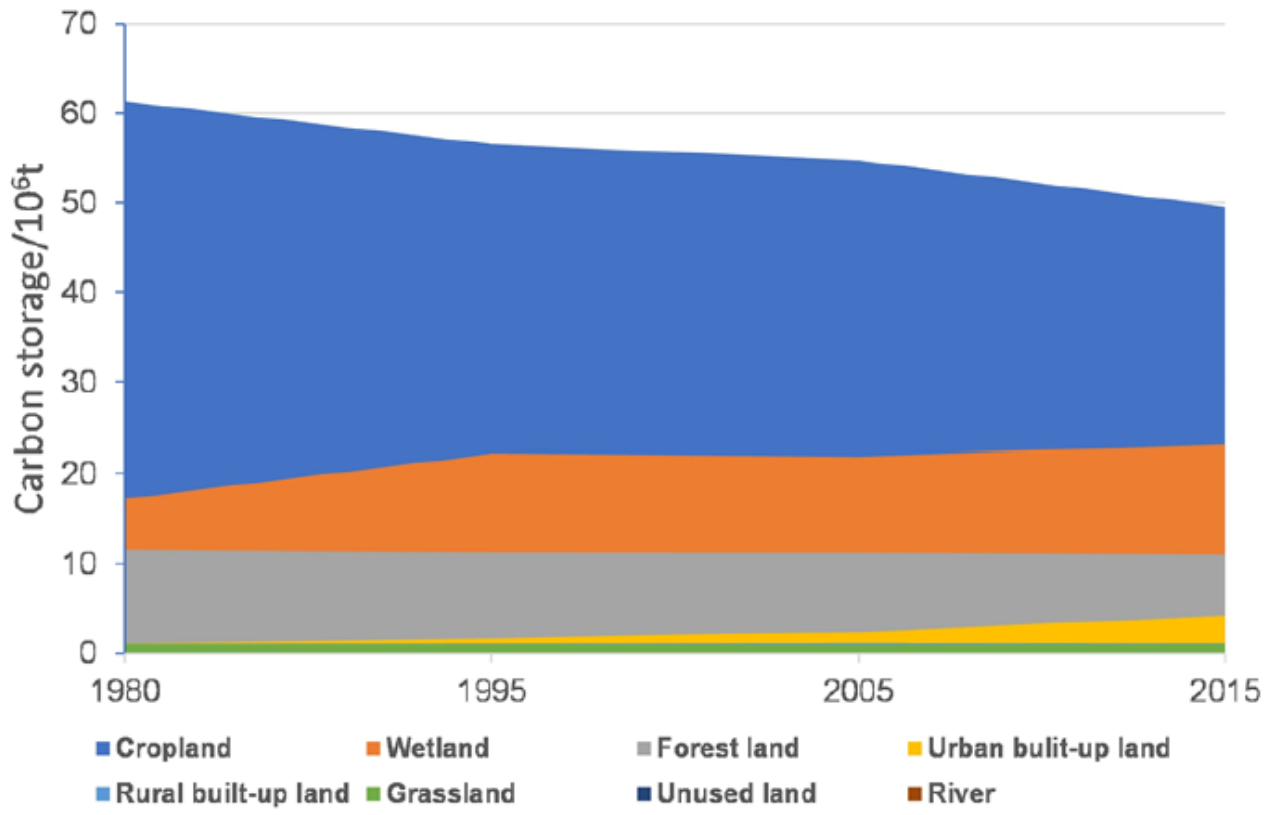


**Figure 8**

Changes in carbon storage of various land use types in Wuhan from 1980 to 2015.

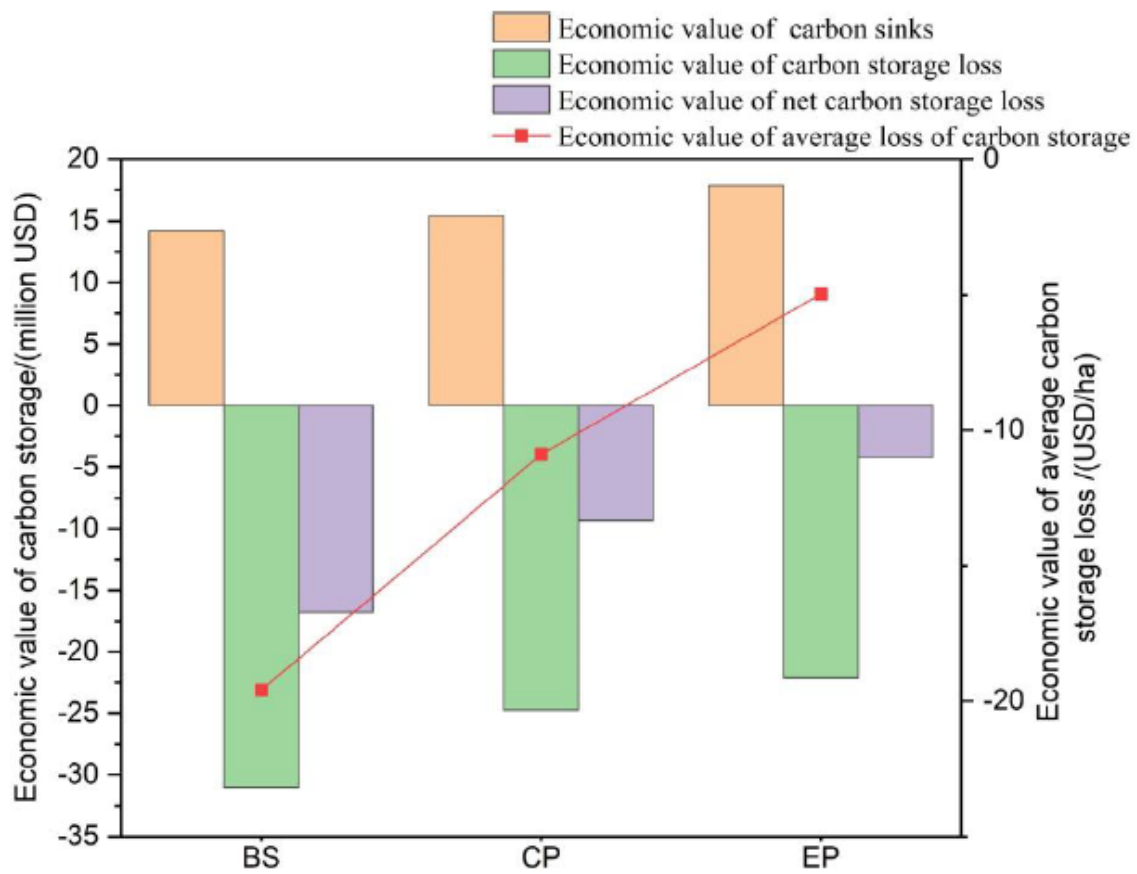


**Figure 9**

Economic value of carbon storage loss under three scenarios in Wuhan, 2035.

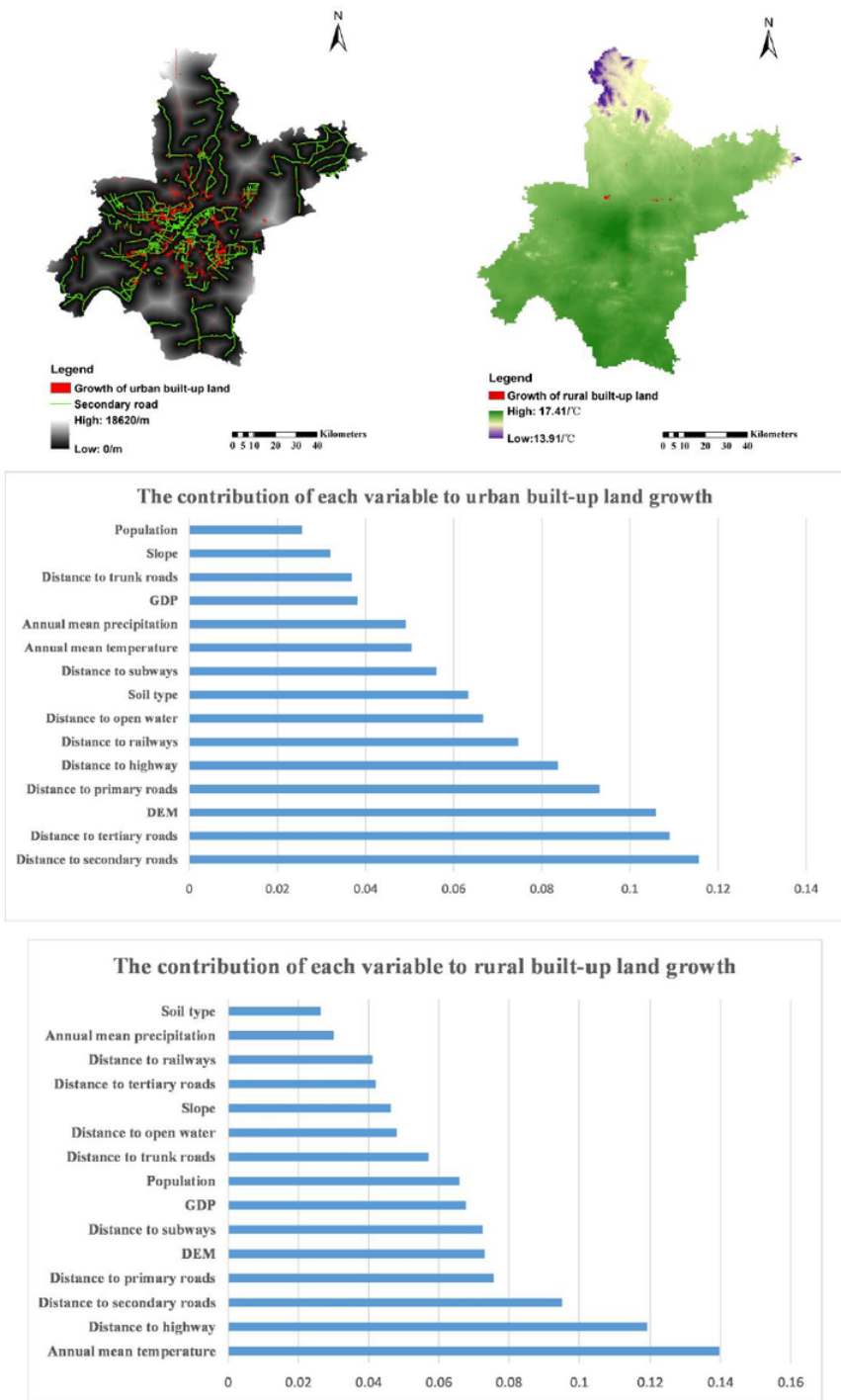


**Figure 10**

Contribution of each drivers to the growth of urban and rural built-up land and the spatial relationship between the most important factors and the expansion of corresponding land use.

## Supplementary Files

This is a list of supplementary files associated with this preprint. Click to download.

- [Appendices.docx](#)